RSC Advances

RSC Publishing

PAPER

View Article Online
View Journal | View Issue

Atomic layer deposition of $Li_xTi_yO_z$ thin films†

Cite this: *RSC Advances*, 2013, **3**, 7537

Ville Miikkulainen,[a] Ola Nilsen,*[a] Mikko Laitinen,[b] Timo Sajavaara[b] and Helmer Fjellvåg[b]

Received 12th February 2013,
Accepted 8th March 2013

DOI: 10.1039/c3ra40745d

www.rsc.org/advances

Atomic layer deposition (ALD) was employed to deposit ternary films of $Li_xTi_yO_z$. The film growth at a deposition temperature of 225 °C was studied using both titanium tetra-isoropoxide ($Ti(O^iPr)_4$) and titanium tetrachloride ($TiCl_4$) as titanium precursors. Lithium *tert*-butoxide (LiO^tBu) was applied as the lithium source and water was used as the oxygen source for all metal precursors. The type of titanium precursor chosen strongly affected film growth: with $TiCl_4$ the resulting $Li_xTi_yO_z$ films were highly air-sensitive and the lithium concentration was low, whereas with $Ti(O^iPr)_4$ the films were relatively stable in air and with a lithium content which was easily controlled over a wide range. Film characterization indicated that part of the lithium in the film migrated onto the surface and formed carbonates. Films with suitable lithium contents crystallized into the spinel $Li_4Ti_5O_{12}$ structure upon post-deposition annealing.

Introduction

Thin film lithium ion batteries offer an improved safety and cycling performance compared to classical lithium ion batteries employing a liquid electrolyte.[1] In classical lithium batteries, a solid electrolyte interface (SEI) layer is formed as the battery is cycled. The formation is frequently irreversible and reduces the capacity and high rate performance of the battery. In addition, dendritic growth of lithium can take place, especially at high current densities, resulting eventually into a short-circuit. In all-solid-state batteries, the formation of both a SEI layer and lithium dendrites is avoided due to the high stability of the solid electrolyte.

Thin film batteries have so far mainly been prepared by physical vapor deposition (PVD) methods, such as magnetron sputtering and pulsed laser deposition.[1] These are line-of-sight methods limiting the film stack to planar geometry. However, if the film stack was deposited onto a three dimensional substrate, the footprint capacity would significantly increase. Realization of such 3D battery structures would, on the other hand, require much thinner electrodes in the form of films. This would again lead to an improved high rate performance due to shorter ionic and electronic diffusion paths.[2–4]

With atomic layer deposition (ALD) highly conformal films can be deposited onto complex three dimensional substrates.[5] Film growth by ALD is based on successive pulses of precursor vapors that react with the surface in a self-limiting manner. The precursor pulses are separated by inert gas or evacuation purges to prevent gas phase reactions. A fully surface controlled growth enables an accurate control over the film thickness and its composition in addition to a highly conformal nature of the deposited films. Recently, ALD has been introduced as an enabling method for all-solid-state 3D lithium ion batteries.[6] The unique properties of ALD exceed the limitations of the state-of-the-art thin film battery fabrication methods. Lithium is obviously a fundamental component of lithium ion batteries, yet the field of lithium containing materials is quite new to ALD as the number of reported processes is limited.[7–13]

Lithium titanate spinel, $Li_4Ti_5O_{12}$ (LTO), has many advantageous properties especially suitable for all-solid-state cells.[14] LTO's cubic $(Li_{1/3}Ti_{5/3})O_4$ framework enables an isotropic lithium diffusion which cancels out the film orientation effects on battery kinetics. Moreover, its volume change upon electrochemical cycling is only 0.3%, which is crucial in a rigid film stack to prevent the film from cracking and peeling off. The intercalation reaction of LTO, yielding a theoretical capacity of 175 mA h g^{-1}, is demonstrated by eqn (1):

$$Li_4Ti_5O_{12} + 3Li^+ + 3e^- \leftrightarrow Li_7Ti_5O_{12} \quad (1)$$

LTO has a lithium insertion potential around 1.55 V *vs.* Li/Li^+ which is constant over a wide capacity range due to a two-phase intercalation mechanism. Owing to these properties, LTO is an attractive material for thin film batteries. Its deposition has previously been demonstrated with several different thin film methods.[15–17] To our knowledge, there are only preliminary reports on $Li_xTi_yO_z$ deposition by ALD.[18–20]

In the present study we combined the TiO_2 and Li_2O–LiOH binary ALD processes to prepare the $Li_xTi_yO_z$ ternary material. For the TiO_2 subcycle we studied the effect of alkoxide and chloride based chemistries on $Li_xTi_yO_z$ growth. We found that

[a]*Centre for Materials Science and Nanotechnology (SMN), Department of Chemistry, University of Oslo, P.O. Box 1126, Blindern, NO-0318 Oslo, Norway. E-mail: ola.nilsen@kjemi.uio.no*

[b]*Department of Physics, FI-40014 University of Jyväskylä, P.O. Box 35, Finland*

† Electronic supplementary information (ESI) available: X-ray photoelectron spectra for $Li_xTi_yO_z$ films. See DOI: 10.1039/c3ra40745d

the chloride-based process yielded low concentrations of lithium in the film, whereas with an alkoxide based process the composition of the film can be controlled over a wide range by altering the Li_2O–LiOH : TiO_2 pulsing ratio. With an appropriate pulsing ratio, the LTO phase was found in the as-deposited film and the crystallinity of the film improved upon annealing.

Experimental

All the depositions were made with an ASM F-120 Sat reactor at a deposition temperature of 225 °C. Titanium tetrachloride ($TiCl_4$, Sigma-Aldrich 99.9%) and titanium tetra-isopropoxide ($Ti(O^iPr)_4$, Aldrich 97%) were used as titanium precursors and used as-received. Titanium tetrachloride was evaporated from an external vessel at room temperature and $Ti(O^iPr)_4$ was evaporated from an external overflow bottle at room temperature. Lithium *tert*-butoxide (LiO^tBu, Aldrich 97%) was employed as the lithium precursor and used without further purification. It was evaporated at 130 °C from an open boat inside the reactor. Glass wool was used in the end of the source tube to prevent light residual solids of the LiO^tBu from flying into the reaction chamber and onto the growing film. Depositions were made on silicon and platinum coated silicon. Nitrogen (99.999% N_2) was used as a carrier and purging gas. Reactor pressure was around 3 mbar during depositions.

Film thicknesses were characterized with spectroscopic ellipsometry (Woollam Alpha SE) by applying the Cauchy model for LTO films. The crystallinity of the films was studied with a Bruker AXS D8 powder diffractometer equipped with a Ge(111) monochromator providing Cu Kα1 radiation and using a LynxEye detector. Compositional analyses were made with both time-of-flight elastic recoil detection analysis (TOF-ERDA) and photoelectron spectroscopy (XPS, Kratos Axis Ultra^{DLD}). In the TOF-ERDA measurements an 8 MeV 35Cl or 79Br beam from a Pelletron accelerator bombarded the sample and the energy spectra of the forward scattered particles were used as the basis of the elemental depth profiles. With TOF-ERDA all the atoms of the samples, including hydrogen, can be quantitatively depth profiled.

Results and discussion

Depositions with titanium tetrachloride as the titanium precursor

First we studied $TiCl_4$ as the titanium source by depositing a series of films on silicon with the pulsing sequence $N \times [A \times \{TiCl_4\ (0.5\ s\ pulse/1\ s\ purge) + H_2O(2/3)\} + 1 \times \{LiO^tBu(8/8) + H_2O(4/8)\}]$, where N and A are whole numbers. The elemental composition and the Li : Ti ratio of the films were quantified by TOF-ERDA. As seen in Fig. 1, the Li : Ti ratio stays at a low level even though the growth per cycle increases as the Li : Ti pulsing ratio ($1/A$) increases. In addition, the films were highly air-sensitive as they reacted rapidly with air when taken out from the ALD reactor. The films became opaque but restored their transparency and uniformity after a few days in air. Characterizations were made on these reacted, uniform films since the immediate reaction of the film material was too rapid to facilitate a proper analysis.

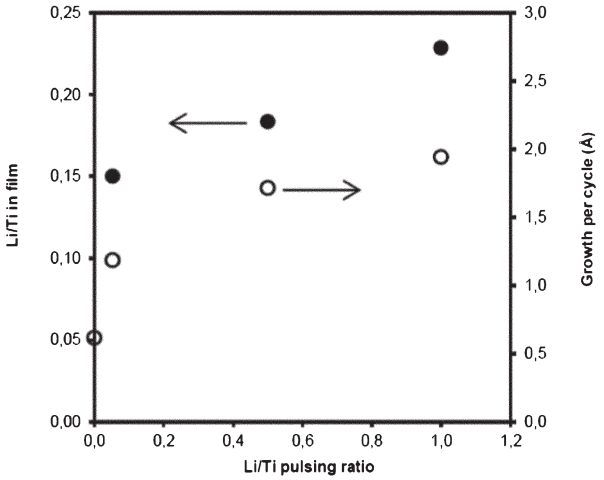

Fig. 1 Film growth per cycle and Li : Ti elemental ratio of the $Li_xTi_yO_z$ films *vs.* the Li : Ti pulsing ratio deposited using $TiCl_4$ as the titanium source. TOF-ERDA data for this figure were provided by Dr. Alexander Azarov at the University of Oslo.

The elemental composition of a 97 nm film deposited with a 1 : 1 Li : Ti pulsing ratio from $TiCl_4$ is tabulated in Table 1. The amount of chlorine is at the same level as reported for pure TiO_2 films deposited from $TiCl_4$ at the temperature of 225 °C.[21] In contrast, the amount of hydrogen and carbon is notable in the film. $Li_xTi_yO_z$ films deposited with $TiCl_4$ were amorphous as studied by XRD.

Aaltonen *et al.* recently published an ALD process for lithium lanthanum titanate (LLT) based on $TiCl_4$–water, LiO^tBu–water and $La(thd)_3$–ozone for TiO_2, LiOH–Li_2O and La_2O_3 subcycles, respectively.[7] In other words, the LLT process employs the same precursor chemistries for TiO_2 and LiOH–Li_2O as our $Li_xTi_yO_z$ process described in the previous paragraphs. In case of LLT, if the lithium subcycle was introduced after the titanium subcycle, the films were less uniform than if the lithium was introduced after the lanthanum subcycle. In the latter case, the films were uniform and air-stable. The lithium concentration was quite high for

Table 1 Elemental composition (TOF-ERDA) of a 97 nm film deposited from $TiCl_4$ with a 1 : 1 Li : Ti pulsing ratio

Element	Atomic % ± error
O	58 ± 4
Ti	23 ± 2
H	8 ± 2
C	5 ± 1
Li	5 ± 1
Cl	1.1 ± 0.2
Na	0.22 ± 0.05
N	<0.1

both cases compared to our findings. Aaltonen *et al.* however, found that the addition of successive lithium subcycles did not increase the lithium content in the films, contrary to what one would expect. It was concluded that the substrate surface is more reactive towards LiO^tBu after a lanthanum subcycle than it is after a lithium subcycle. Similar factors may explain the unexpected low lithium concentrations in the $Li_xTi_yO_z$ films employing $TiCl_4$ as well.

Since lithium was found to be difficult to incorporate into the film and the films were air-sensitive, further studies on $Li_xTi_yO_z$ depositions employing $TiCl_4$ as a titanium source were postponed at this point.

Depositions with titanium tetra-isopropoxide as the titanium precursor

A similar study was done using titanium tetra-isopropoxide ($Ti(O^iPr)_4$) as the titanium source and a pulsing sequence of $N \times [A \times \{Ti(O^iPr)_4(10\text{ s pulse}/5\text{ s purge}) + H_2O(1/5)\} + B \times \{LiO^tBu(8/12) + H_2O(1/8)\}]$, where N, A and B are whole numbers. The Li : Ti ratio obtained with TOF-ERDA for these films and the growth per cycle are presented in Fig. 2. Rather long $Ti(O^iPr)_4$ pulses were required to achieve good uniform films. If the pulse length was shortened, the $Li_xTi_yO_z$ films were much thicker, milky and non-uniform. The films with an insufficient $Ti(OiPr)_4$ pulse time also reacted with ambient air within the time scale of days. The unsaturating conditions of the titanium isopropoxide pulse probably lead to highly lithium rich films which are hygroscopic. Water physisorption into such a hygroscopic material during water pulses can eliminate the self-limiting nature of film growth. In addition, the $Ti(O^iPr)_4$ vapor concentration is quite low in our source system because the vapor pressure of $Ti(O^iPr)_4$ is about 0.1 Torr at room temperature. Usually titanium isopropoxide is heated to 40–50 °C achieving a vapor pressure of 0.4–0.9 Torr.[22] On the other hand, our source design enables an easier handling of the precursor.

The hygroscopic nature of lithium-containing ALD films has been frequently reported.[7,9,11,13] For Li–Al–O films it was observed that water physisorbs rather heavily into the growing film even when used as a precursor.[9] *In situ* quartz crystal microbalance analysis showed that if the purge time after the water pulse was elongated, the amount of water decreased but was not completely removed within a reasonable purging time. Nevertheless, the self-limiting nature of film growth was verified and a seemingly small amount of physisorbed water is allowed to still maintain the surface-controlled growth.[9]

For the same pulsing ratios, the lithium content in the film is much higher with the $Ti(O^iPr)_4$-based process than with the $TiCl_4$-based one, as can be seen from Fig. 1 and 2. At the same time, growth per cycle does not increase for the $Ti(O^iPr)_4$-based process as much as for the chloride-based process when the Li : Ti pulsing ratio is increased. It should also be noted that the lithium concentration range accessible with the $Ti(O^iPr)_4$-based process is wide. The film uniformity was very good regardless of the lithium concentration. These films react with air as well, but within a time ranging from weeks to months depending on lithium concentration. Films became milky starting from the edges upon reaction with air.

To verify the surface-controlled, self-limiting nature of film growth, the pulse saturation of LiO^tBu was studied. The pulsing sequence was $N \times [2 \times \{Ti(O^iPr)_4(10\text{ s pulse}/5\text{ s purge}) + H_2O(1/5)\} + \{LiO^tBu(X/12) + H_2O(1/8)\}]$. The pulse length was varied and the growth per cycle and lithium concentration were characterized. Pulse saturation results are shown in Fig. 3, proving a saturation of the LiO^tBu pulse close to four seconds, which is lower than the eight second pulses applied throughout the study.

Characterization of $Li_xTi_yO_z$ films deposited from titanium tetra-isopropoxide

Compositional analysis with TOF-ERDA

Besides the Li : Ti ratios and Li concentration presented in Fig. 1–3, TOF-ERDA was employed for the detailed composi-

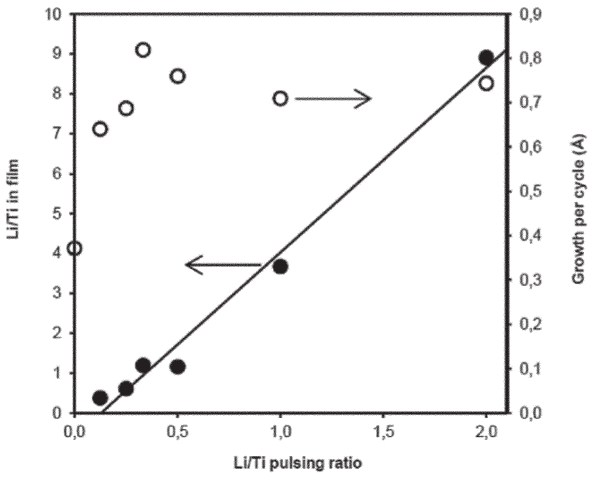

Fig. 2 Film growth per cycle and the Li : Ti TOF-ERDA elemental ratio of $Li_xTi_yO_z$ films *vs.* the Li : Ti pulsing ratio deposited using $Ti(OiPr)_4$ as the titanium source. The line corresponds to the linear fit of the Li : Ti ratio in the film *vs.* the Li : Ti pulsing ratio.

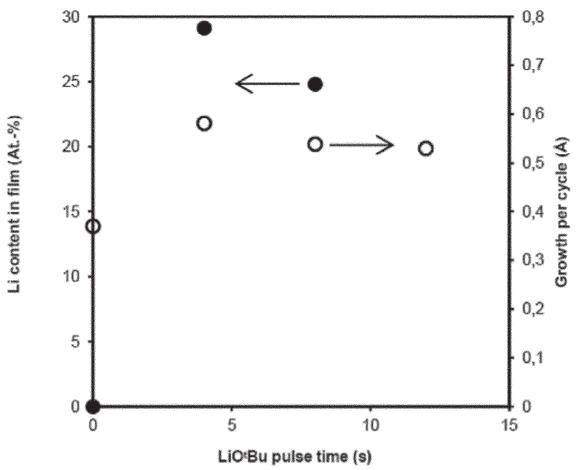

Fig. 3 Lithium content (TOF-ERDA) and growth per cycle of a $Li_xTi_yO_z$ film deposited with $Ti(O^iPr)_4$ as the titanium source (1 : 2 Li : Ti pulsing ratio) as a function of the LiO^tBu pulse time

Table 2 TOF-ERDA elemental compositions for $Li_xTi_yO_z$ sample films deposited with three different pulsing ratios

	Concentration (atomic %) ± error		
Element	1 : 8 Li : Ti puls.	1 : 2 Li : Ti puls.	2 : 1 Li : Ti puls.
Ti	28 ± 1	21 ± 1	3.2 ± 0.3
Li	10 ± 1	25 ± 1	28 ± 2
O	58 ± 3	52 ± 2	48 ± 3
H	3.0 ± 0.5	1.7 ± 0.2	5.5 ± 1.0
C	0.5 ± 0.2	0.09 ± 0.05	14 ± 2
N	<0.05	<0.05	—
Na	0.07 ± 0.04	0.18 ± 0.04	0.5 ± 0.1

tional analysis and depth profiling. In Table 2, the elemental composition of samples with three selected Li : Ti pulsing ratios are presented. As can be seen, the carbon content is very low for the 1 : 8 and 1 : 2 pulsing ratios considering the low deposition temperature and carbon-rich ligand sphere. The hydrogen content is also low for those two pulsing ratios. The amount of oxygen in the film is in line with the titanium and lithium concentrations for 1 : 8 and 1 : 2 pulsing ratio films whereas the 2 : 1 film shows oxygen concentrations much higher than expected from the metal concentrations. Also, both the carbon and hydrogen concentrations are much higher in the film with the highest lithium concentration.

The oxygen off-stoichiometry and the high levels of contamination concentrations may be due to either the less favorable chemistry at a high Li : Ti pulsing ratio, leaving unreacted ligands in the film during its growth, or the increased reactivity of the film towards air. The sodium concentration increases along with the lithium concentration and most probably originates from impurities in the LiO^tBu precursor. The sodium content is however low even in the film with the highest lithium content.

The elemental depth profile for an 89 nm film deposited with a 1 : 2 Li : Ti pulsing ratio is presented in Fig. 4. The bulk of the film is homogeneous with respect to all its constituent elements. The carbon concentration is very low inside the film but clearly peaks on the film surface. Hydrogen is also enriched on the surface.

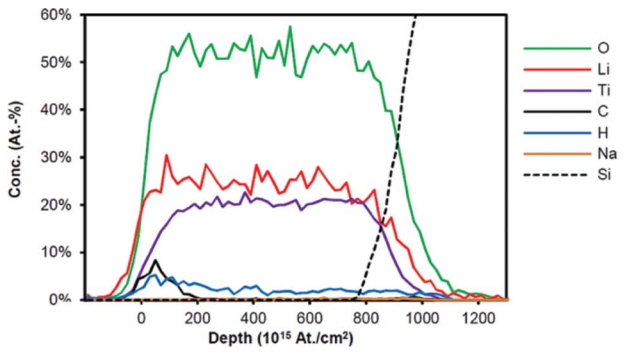

Fig. 4 Elemental TOF-ERDA depth profile of an 89 nm film deposited with a 1 : 2 Li : Ti pulsing ratio on silicon.

Surface analysis with X-ray photoelectron spectroscopy (XPS)

By studying the film surface with XPS one would obtain detailed information on the chemical states of the film surface components. XPS is a very surface sensitive method with a probing depth of only a few nanometers. The surface spectra were collected for the two $Li_xTi_yO_z$ films made with both of the titanium precursors while a commercial LTO nanopowder (<100 nm particle size, Aldrich >99%) was used as a reference. The $TiCl_4$- and $Ti(O^iPr)_4$-originated samples were made with 1 : 2 and 1 : 9 pulsing ratios, respectively. All the measured spectra can be found in the supplementary material. As reported by Dedryvère *et al.*, carbonates on the $Li_4Ti_5O_{12}$ surface show C1s and O1s peaks at 290.0 eV and 532.0 eV, respectively.[23] Among the samples we studied, the LTO reference shows a very low intensity throughout the C1s region, 294–282 eV. The $TiCl_4$-originated $Li_xTi_yO_z$ film gives peaks with notable intensities at 289.1, 286.5 and 285.5 eV. These can be addressed to the organic carbons in the CH_2, C–O and O–C=O environments, respectively.[23] These are most probably from both the residuals of the ligands of the ALD precursors during film growth and the hydrocarbons from ambient air. In the spectrum of the $Ti(O^iPr)_4$-based $Li_xTi_yO_z$ film, there is a significant peak of carbonate at 289.8 eV in addition to those three other carbon peaks. In the O1s regions of the spectra, the carbonate peak at 532.0 eV is very low for the reference and the $TiCl_4$-originated film but significant for the $Ti(O^iPr)_4$-originated film. Actually, the carbonate peak is more intense than the metal oxide peak at 529.5 eV. It seems plausible that the carbonate on top of the film is a result of the film reacting with ambient carbon dioxide since the carbon content inside the film is very low and the carbon is heavily concentrated on the topmost surface in the form of carbonates.

Li : Ti concentration ratios were also studied with XPS similarly to what was done with TOF-ERDA. Quantifications were based on the Li1s, O1s, and Ti2p peak integrals. The LTO reference sample gave a stoichiometry of $Li_{4.1}Ti_{5.0}O_{12}$ validating the quantification method. Li : Ti ratios obtained for the ALD-films differed from the values based on TOF-ERDA data. For the $TiCl_4$-originated film, XPS gave a Li : Ti ratio of 0.48 while the Li : Ti ratio for the $Ti(O^iPr)_4$-based film was 1.82. These values are much higher than the corresponding values obtained from the film bulk with TOF-ERDA shown in Fig. 1 and 2 (0.18 and 0.3, respectively). This supports the conclusion that lithium is enriched on top of the film. The same effect is found with both ALD chemistries. The magnitude of the enrichment seems to be much higher in the case of $Ti(O^iPr)_4$ but there are probably several other parameters than just the precursor chemistry influencing it. These may include the overall lithium concentration in the film and exposure time to ambient air, among others.

The amount of carbonates and the lithium enrichment were both found to be low for the powder reference. Lack of a lithium enrichment is most probably due to the stoichiometric and polycrystalline nature of the material. In less ordered, off-stoichiometric structures of the ALD materials the lithium ions are most likely more mobile than in the polycrystalline $Li_4Ti_5O_{12}$ reference.

X-Ray diffraction (XRD)

For the $Li_xTi_yO_z$ films to be applied as battery electrodes, the lithium titanate spinel (LTO) crystalline phase needs to be formed in order to obtain the expected electrochemical properties. We studied the film crystallinity with XRD in θ–2θ mode in the angle range between 10 and 80 degrees.

Silicon is well-known for its redox reactions with lithium ions.[24] Therefore a diffusion barrier, such as platinum, is needed between the silicon substrate and the LTO films to prevent silicon from reacting with the lithium ions if the electrochemical studies are conducted on the sample. Films were deposited on platinum coated silicon also for XRD analysis to have a good correlation between the film microstructure and the electrochemical characteristics. Platinum is also a widely applied current collector for battery electrodes. The sample was a 110 nm film deposited using a 2 : 3 Li : Ti pulsing ratio which should yield a deposited Li : Ti ratio of 1.5 (Fig. 2). This is higher than the 0.8 expected for stoichiometric LTO. A higher value for the Li : Ti ratio was selected to compensate for the lithium diffusion onto the surface and carbonate formation as well as possible lithium loss during annealing. X-Ray diffractograms for as-deposited and annealed films are presented in Fig. 5. The annealing was performed in a rapid thermal processing (RTP) oven (MTI corporation, USA) under a nitrogen atmosphere for five seconds.

For all of the three studied samples, the only crystalline phase arising from the film is spinel LTO. Neither rutile nor anatase, the most common impurities in LTO syntheses,[25,26] are visible. The LTO reflections become stronger when the film is annealed indicating film crystallization. The film is somewhat [100] oriented since (111) would be the strongest reflection in the powder standard 49-0207. Films prepared by other methods have been reported to be [111] oriented.[15–17]

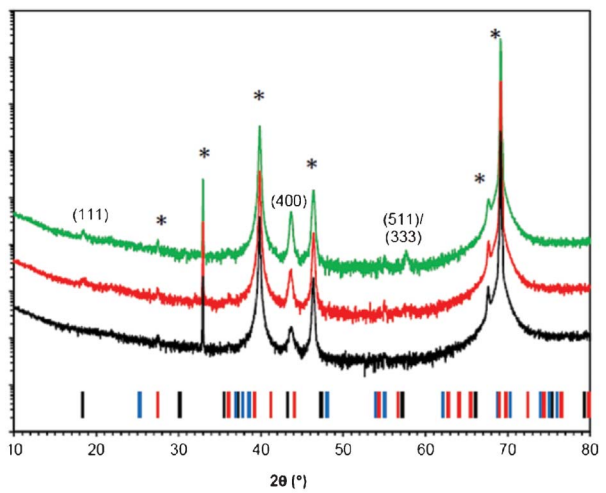

Fig. 5 X-ray diffractograms for as-deposited (black, bottom), 640 °C annealed (red, middle), and 700 °C annealed films (green, top). The black tick-marks below the graphs correspond to spinel $Li_4Ti_5O_{12}$ (JCPDS 49-0207), the blue to anatase TiO_2 (JCPDS 21-1272) and the red to rutile TiO_2 (JCPDS 01-078-2485). Indexing refers to spinel $Li_4Ti_5O_{12}$. Reflections from the substrate are marked with an asterisk.

Conclusions

In the present study, ALD processes for lithium titanium oxide ($Li_xTi_yO_z$) films were studied at the deposition temperature of 225 °C by combining LiO^tBu–H_2O process with two different titanium oxide processes. By combining $Ti(O^iPr)_4$ with lithium oxide process, the lithium concentration could be readily controlled with a Li_2O–LiOH : TiO_2 pulsing ratio. The accessible composition range was wide and the films were also relatively stable towards air. Films were found to form carbonates onto the surface. Post-deposition annealing crystallized the film with a suitable composition into the LTO spinel phase. With the ALD–LTO process it should be possible to deposit lithium titanate films as anodes for 3D battery architectures. Studies are ongoing to characterize the electrochemical properties of the ALD–LTO material.

Notes and references

1 N. J. Dudney, *Interface*, 2008, **17**, 44.
2 J. W. Long, B. Dunn, D. R. Rolison and H. S. White, *Chem. Rev.*, 2004, **104**, 4463.
3 J. F. M. Oudenhoven, L. Baggetto and P. H. L. Notten, *Adv. Energy Mater.*, 2011, **1**, 10.
4 M. Roberts, P. Johns, J. Owen, D. Brandell, K. Edström, G. El Enany, C. Guery, D. Golodnitsky, M. Lacey, C. Lecoeur, H. Mazor, E. Peled, E. Perre, M. M. Shaijumon, P. Simon and P.-L. Taberna, *J. Mater. Chem.*, 2011, **21**, 9876.
5 C. Detavernier, J. Dendooven, S. Pulinthanathu Sree, K. F. Ludwig and J. A. Martens, *Chem. Soc. Rev.*, 2011, **40**, 5242.
6 P. H. L. Notten, F. Roozeboom, R. A. H. Niessen and L. Baggetto, *Adv. Mater.*, 2007, **19**, 4564.
7 M. Putkonen, T. Aaltonen, M. Alnes, T. Sajavaara, O. Nilsen and H. Fjellvåg, *J. Mater. Chem.*, 2009, **19**, 8767.
8 T. Aaltonen, M. Alnes, O. Nilsen, L. Costelle and H. Fjellvåg, *J. Mater. Chem.*, 2010, **20**, 2877.
9 T. Aaltonen, O. Nilsen, A. Magrasó and H. Fjellvåg, *Chem. Mater.*, 2011, **23**, 4669.
10 M. Donders, H. C. M. Knoops, W. M. M. Kessels and P. H. L. Notten, *ECS Trans.*, 2011, **41**, 321.
11 J. Hämäläinen, J. Holopainen, F. Munnik, T. Hatanpää, M. Heikkilä, M. Ritala and M. Leskelä, *J. Electrochem. Soc.*, 2012, **159**, A259.
12 J. Hämäläinen, F. Munnik, T. Hatanpää, J. Holopainen, M. Ritala and M. Leskelä, *J. Vac. Sci. Technol., A*, 2012, **30**, 01A106.
13 E. Østreng, P. Vajeeston, O. Nilsen and H. Fjellvåg, *RSC Adv.*, 2012, **2**, 6315.
14 T.-F. Yi, L.-J. Jiang, J. Shu, C.-B. Yue, R.-S. Zhu and H.-B. Qiao, *J. Phys. Chem. Solids*, 2010, **71**, 1236.
15 J. Deng, Z. Lu, I. Belharouak, K. Amine and C. Chung, *J. Power Sources*, 2009, **193**, 816.
16 C.-L. Wang, Y. C. Liao, F. C. Hsu, N. H. Tai and M. K. Wu, *J. Electrochem. Soc.*, 2005, **152**, A653.
17 Y. H. Rho, K. Kanamura, M. Fujisaki, J. ichi Hamagami, S. ichi Suda and T. Umegaki, *Solid State Ionics*, 2002, **151**, 151.
18 T. Aaltonen, V. Miikkulainen, K. B. Gandrud, A. Pettersen, O. Nilsen and H. Fjellvåg, *ECS Trans.*, 2011, **41**, 331.

19 D. J. Comstock and J. W. Elam, *presented in part at the 11th AVS-ALD Meeting*, Boston, June, 2011.
20 X. Meng, *Ph.D. Thesis*, The University of Western Ontario, 2011.
21 M. Ritala and M. Leskelä, *Thin Solid Films*, 1993, **225**, 288.
22 M. Ritala, M. Leskelä, L. Niinistö and P. Haussalo, *Chem. Mater.*, 1993, **5**, 1174.
23 R. Dedryvére, D. Foix, S. Franger, S. Patoux, L. Daniel and D. Gonbeau, *J. Phys. Chem. C*, 2010, **114**, 10999.
24 C. K. Chan, H. Peng, G. Liu, K. McIlwrath, X. F. Zhang, R. A. Huggins and Y. Cui, *Nat. Nanotechnol.*, 2008, **3**, 31.
25 Y. Hao, Q. Lai, D. Liu, Z. Xu and X. Ji, *Mater. Chem. Phys.*, 2005, **94**, 382.
26 S.-H. Yu, A. Pucci, T. Herntrich, M.-G. Willinger, S.-H. Baek, Y.-E. Sung and N. Pinna, *J. Mater. Chem.*, 2011, **21**, 806.